Mode-partition noise and intensity correlation in a two-mode semiconductor laser

Govind P. Agrawal

AT&T Bell Laboratories, Murray Hill, New Jersey 07974-2070

The intensity-noise characteristics of a nearly single-longitudinal-mode semiconductor laser are analyzed by adopting a two-mode model. An approximate solution of the resulting Langevin rate equations is used to obtain an analytic expression for the enhancement of the main-mode intensity noise caused by mode partition. We also obtain analytic expressions for the autocorrelation and cross-correlation functions which are used to discuss noise variances in the two modes. In particular, the cross-correlation function is related to the mode-partition coefficient, a measure of anticorrelation between the two modes that is useful to analyze the system performance. Our results show explicitly how the intensity correlation is affected by the mode-suppression ratio and other device parameters.

I. INTRODUCTION

The performance of an optical communication system employing multimode semiconductor lasers is strongly influenced by mode partition, a phenomenon which enhances the intensity noise of individual longitudinal modes even though the total intensity noise remains relatively small.[1-14] Although it has been realized that mode-partition noise is due to an anticorrelation among the longitudinal modes, the evaluation of the intensity-correlation coefficients is generally difficult for a multimode semiconductor laser owing to the complexity of the problem. As a result, the effect of mode-partition noise on the system performance is analyzed[15] by introducing a phenomenological parameter known as the mode-partition coefficient k. Since the dependence of k on the laser parameters is not known, it is treated as a fitting parameter or determined experimentally.[15] Recently attempts have been made[11-13] to measure and evaluate k for distributed feedback lasers in order to quantify the importance of mode-partition noise for single-frequency lightwave systems operating at 1.55 μm.[7,10]

The objective of this paper is to consider the noise characteristics of a nearly single-longitudinal-mode semiconductor laser by adopting a two-mode model. This allows us to obtain an analytic expression for the intensity-noise enhancement of the dominant mode cause by mode partition. Our approach is similar to that of Henry *et al.*[4] except that we consider the rate equations for the main and side modes on the same footing without using the process of adiabatic elimination. The inclusion of only two modes allows us to obtain the analytic forms for both the autocorrelation and cross-correlation functions. The latter can be used to obtain an expression for the mode-partition coefficient k. Our results show that mode-partition coefficient depends on the damping rate of side-mode fluctuations that is affected by the nonlinear-gain suppression[16-18] occurring due to phenomena such as spectral hole burning.

II. LANGEVIN EQUATIONS

In the Langevin formulation of the laser-noise analysis[19-21] the rate equations governing laser dynamics are supplemented with fluctuating noise sources. In the case of a two-mode laser the resulting Langevin equations are[22]

$$\dot{P} = (G_1 - \gamma_1)P + R_{sp} + F_p(t) , \qquad (1)$$

$$\dot{S} = (G_2 - \gamma_2)S + R_{sp} + F_s(t) , \qquad (2)$$

$$\dot{N} = I/q - \gamma_e N - (G_1 P + G_2 S) + F_n(t) , \qquad (3)$$

where P and S are the number of photons in the main mode and the side mode, respectively, and N represents the number of carriers (electrons or holes) inside the active region of the semiconductor laser. We emphasize that P and S are used simply as a dimensionless measure of the mode intensities in the semiclassical description adopted here. The rate of spontaneous emission R_{sp} is assumed to be the same for the two modes as the mode separation is generally much smaller compared to the width of the spontaneous-emission spectrum. G_1 and γ_1 represent the rate of stimulated emission (net gain) and the cavity decay rate (net loss) for the main mode while G_2 and γ_2 are the corresponding quantities for the side mode. In (3) I is the injected current and γ_e is the carrier recombination rate near threshold. In general γ_e is a function of N to account for the processes such as Auger recombination. The Langevin noise sources $F_p(t)$, $F_s(t)$, and $F_n(t)$ are responsible for fluctuations in P, S, and N, respectively. In the Markoffian approximation[20] they satisfy

$$\langle F_i(t) \rangle = 0 , \qquad (4)$$

$$\langle F_i(t)F_j(t') \rangle = 2D_{ij}\delta(t - t') , \qquad (5)$$

where $i,j = p$, s, and n. The diffusion coefficients D_{ij} are given by[21,22]

$$D_{pp} = R_{sp}\bar{P}, \quad D_{ss} = R_{sp}\bar{S}, \quad D_{ps} = 0 , \tag{6}$$

$$D_{nn} = R_{sp}(\bar{P} + \bar{S}) + \gamma_e \bar{N}, \quad D_{pn} = -R_{sp}\bar{P}, \quad D_{sn} = -R_{sp}\bar{S} , \tag{7}$$

where $\bar{P}$, $\bar{S}$, and $\bar{N}$ denote the average values.

To complete the description, the dependence of the mode gains G_1 and G_2 on P, S, and N should be known. Assuming that the gain varies linearly with N, we take

$$G_1 = A(N - N_0) - \beta_{11}P - \theta_{12}S , \tag{8}$$

$$G_2 = A(N - N_0) - \beta_{22}S - \theta_{21}P - \delta G , \tag{9}$$

where A is the gain coefficient, N_0 is the carrier population required for transparency, and δG is the reduction in the side-mode gain due to gain roll off. The dependence of the gain on the photon populations P and S is due to nonlinear phenomena such as spectral hole burning which result in gain saturation.[16-18] For a two-mode laser, it is important to include both the self-saturation and cross-saturation terms governed by β_{ii} and θ_{ij} ($i,j = 1,2$), respectively. In particular, as seen below, cross saturation enhances considerably the decay rate of side-mode fluctuations.

The Langevin equations (1)–(3) are solved in the quasi-linear approximation[19-22] wherein Eqs. (1)–(3) are linearized in terms of small fluctuations $p(t)$, $s(t)$, and $n(t)$ occurring around the steady-state values $\bar{P}$, $\bar{S}$, and $\bar{N}$, respectively. This leads to the following set of Langevin equations (for brevity, the overbar is omitted for steady-state variables):

$$\dot{p} = -\Gamma_p p + (AP)n - (\theta_{12}P)s + F_p(t) , \tag{10}$$

$$\dot{s} = -\Gamma_s s + (AS)n - (\theta_{21}S)p + F_s(t) , \tag{11}$$

$$\dot{n} = -\Gamma_n n - G_1 p - G_2 s + F_n(t) , \tag{12}$$

where

$$\Gamma_p = R_{sp}/P + \beta_{11}P , \tag{13}$$

$$\Gamma_s = R_{sp}/S + \beta_{22}S , \tag{14}$$

$$\Gamma_n = \gamma_e + (d\gamma_e/dN)N + A(P + S) \tag{15}$$

are the decay rates of the fluctuations p, s, and n, respectively. Note that Γ_p and Γ_s are enhanced by the nonlinear-gain mechanism. Note also that cross saturation leads to a direct coupling between the main and side modes.

III. MODE-PARTITION NOISE

In this section we obtain the intensity-noise spectra for fluctuations in the individual mode intensities P and S as well as for the total intensity $P + S$. For this purpose, the Langevin equations (10)–(12) are solved in the Fourier domain using

$$p(t) = \frac{1}{2\pi} \int_{-\infty}^{\infty} \tilde{p}(\omega)\exp(i\omega t)d\omega \tag{16}$$

and similar relations for other time-dependent quantities.

This procedure results in the following set of algebraic equations:

$$(\Gamma_p + i\omega)\tilde{p} + (\theta_{12}P)\tilde{s} - (AP)\tilde{n} = \tilde{F}_p , \tag{17}$$

$$(\Gamma_s + i\omega)\tilde{s} + (\theta_{21}S)\tilde{p} - (AS)\tilde{n} = \tilde{F}_s , \tag{18}$$

$$(\Gamma_n + i\omega)\tilde{n} + G_1\tilde{p} + G_2\tilde{s} = \tilde{F}_n . \tag{19}$$

Equations (17) and (18) are readily solved to obtain

$$\tilde{p} = \frac{(\Gamma_s + i\omega)\tilde{F}_p - \theta_{12}P\tilde{F}_s + AP(\Gamma_s + i\omega - \theta_{12}S)\tilde{n}}{(\Gamma_p + i\omega)(\Gamma_s + i\omega) - \theta_{12}\theta_{21}PS} , \tag{20}$$

$$\tilde{s} = \frac{(\Gamma_p + i\omega)\tilde{F}_s - \theta_{21}S\tilde{F}_p + AS(\Gamma_p + i\omega - \theta_{21}P)\tilde{n}}{(\Gamma_p + i\omega)(\Gamma_s + i\omega) - \theta_{12}\theta_{21}PS} . \tag{21}$$

By substituting $\tilde{p}$ and $\tilde{s}$ in (19), we obtain $\tilde{n}$ in terms of the three Langevin forces. The use of $\tilde{n}$ in (20) and (21) then provides $\tilde{p}$ and $\tilde{s}$ in terms of $\tilde{F}_p$, $\tilde{F}_s$, and $\tilde{F}_n$. Since the resulting expressions are cumbersome, we simplify them by making the following approximations: (i) $\tilde{F}_n$ can be neglected; (ii) the terms proportional to θ_{12} and θ_{21} can be neglected in (20) and (21); and (iii) G_1 and G_2 can be approximated by $G = A(N - N_0) = \gamma_1$ in (19). These approximations amount to keeping the dominant contribution to the intensity noise; the contribution of neglected terms is estimated to be $\sim 1\%$ or less as long as $S/P < 0.2$. The approximate result for $\tilde{p}$ and $\tilde{s}$ is

$$\tilde{p}(\omega) = \frac{\Gamma_n + i\omega}{D(\omega)}\tilde{F}_p - \frac{GAP}{D(\omega)(\Gamma_s + i\omega)}\tilde{F}_s , \tag{22}$$

$$\tilde{s}(\omega) = \frac{1}{\Gamma_s + i\omega}\tilde{F}_s - \frac{GAS}{D(\omega)(\Gamma_s + i\omega)}\tilde{F}_p , \tag{23}$$

where

$$D(\omega) = (\Gamma_n + i\omega)(\Gamma_p + i\omega) + GAP \tag{24}$$

$$= (\Omega_R + \omega - i\Gamma_R)(\Omega_R - \omega + i\Gamma_R) . \tag{25}$$

In (25) we have introduced the angular frequency Ω_R and the decay rate Γ_R of relaxation oscillations by defining

$$\Omega_R = [(GAP + \Gamma_n\Gamma_p) - \Gamma_R^2]^{1/2} , \tag{26}$$

$$\Gamma_R = (\Gamma_n + \Gamma_p)/2 . \tag{27}$$

The relative intensity noise (RIN) for the main and side modes is obtained by using (22) and (23) and by noting that

$$\langle \tilde{F}_i(\omega)\tilde{F}_j^*(\omega) \rangle = 2D_{ij} \quad (i,j = p,s) \tag{28}$$

with D_{ij} given by (6). The result is

$$\frac{\langle |\tilde{p}(\omega)|^2 \rangle}{P^2}$$

$$= \frac{2R_{sp}(\Gamma_n^2 + \omega^2)}{P|D(\omega)|^2}\left[1 + \frac{\Omega_R^4}{(\Gamma_n^2 + \omega^2)(\Gamma_s^2 + \omega^2)}\frac{S}{P}\right] , \tag{29}$$

$$\frac{\langle |\tilde{s}(\omega)|^2 \rangle}{S^2} = \frac{2R_{sp}}{S(\Gamma_s^2 + \omega^2)}\left[1 + \frac{\Omega_R^4}{|D(\omega)|^2}\frac{S}{P}\right] , \tag{30}$$

TABLE I. Parameter values for a 1.55-μm InGaAsP laser operating at 2 mW with a mode-suppression ratio of 100.

Parameter	Symbol	Value
Number of photons in the main mode	P	1.03×10^5
Number of photons in the side mode	S	1.03×10^3
Number of carriers in the active region	N	1.91×10^8
Recombination rate of carriers	γ_e	4.70×10^9 s^{-1}
Decay rate of main-mode photons	γ_1	6.75×10^{11} s^{-1}
Rate of spontaneous emission	R_{sp}	1.35×10^{12} s^{-1}
Gain coefficient	A	7.50×10^3 s^{-1}
Threshold gain	G	6.75×10^{11} s^{-1}
Nonlinear-gain parameter	β	5.40×10^4 s^{-1}
Decay rate of main-mode fluctuations	Γ_p	5.63×10^9 s^{-1}
Decay rate of side-mode fluctuations	Γ_s	1.36×10^9 s^{-1}
Decay rate of carrier fluctuations	Γ_n	1.70×10^9 s^{-1}
Frequency of relaxation oscillations	ν_R	3.64 GHz
Decay rate of relaxation oscillations	Γ_R	3.67×10^9 s^{-1}

where we have used $GAP \simeq \Omega_R^2$ from (26). The term inside the large parentheses represents the enhancement in RIN of an individual mode caused by mode partition. As expected, the enhancement depends on the mode-suppression ratio exhibited by the device.

We have evaluated (29) and (30) using typical parameter values for a 1.55-μm InGaAsP laser. The strongly index-guided laser has active-layer dimensions of $250 \times 2 \times 0.2$ μm^3 and an internal loss of 50 cm^{-1}. The carrier recombination rate γ_e is calculated using a nonradiative recombination time of 10 ns, the spontaneous recombination coefficient of 1×10^{-10} cm^3/s, and the Auger recombination coefficient of 5×10^{-29} cm^6/s. The inclusion of nonlinear-gain terms in (8) and (9) requires that in general four parameters governing self-saturation and cross-saturation should be specified. For simplicity, we assume that $\beta_{11} = \beta_{22} = \beta$ and $\theta_{12} = \theta_{21} = \theta$. This amounts to neglecting a small asymmetry in the nonlinear gain.[17,18] The cross-saturation parameter θ in general depends on the mode separation. For a mode separation of $\lesssim 2$ nm, $\theta \simeq \beta$. Here we assume that $\theta = \beta$. The value of β is estimated using a nonlinear-gain suppression of about 1% per mW of the output power. In particular, the nonlinear-gain parameter ϵ of Ref. 16 is taken to be $\epsilon = 2 \times 10^{-17}$ cm^3. Table I lists the parameter values for a laser operating at 2 mW with a mode-suppression ratio of 100.

The RIN for the main and side modes is shown in Fig. 1 for three values of the intensity ratio S/P. For $S/P = 10^{-5}$, the side-mode contribution to the main-mode RIN is negligible. The corresponding curve in Fig. 1 shows the expected behavior for a single-mode laser together with the relaxation-oscillation peak at $\omega = \Omega_R$. For $S/P > 10^{-3}$ the effect of a weak side mode is to significantly enhance the low-frequency noise ($\omega \ll \Omega_R$); RIN is enhanced by more than 25 dB for $S/P = 0.01$. This enhancement can be seen in (29) where the enhancement factor at low frequencies is $(\Omega_R^2 / \Gamma_n \Gamma_s)^2 (S/P)$. Since $\Omega_R \gg \Gamma_n$ and Γ_s, even a small increase in S/P results in a considerable enhancement of RIN.
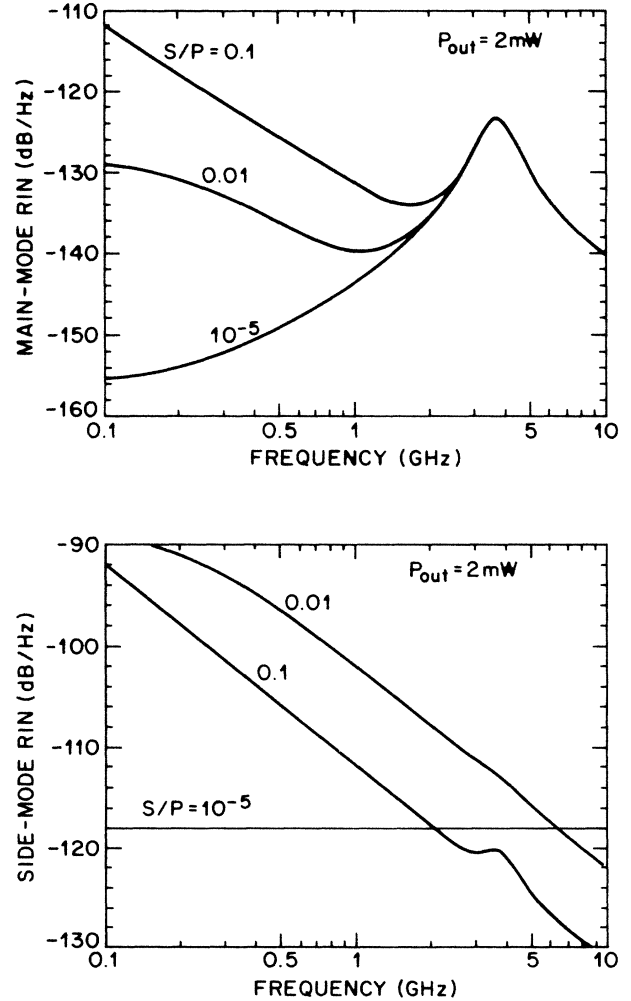

FIG. 1. Relative-intensity-noise (RIN) spectra for the main mode (upper figure) and the side mode (lower figure) for three values of the relative side-mode power S/P. The semiconductor laser is assumed to operate continuously at 2 mW with parameters given in Table I.

The RIN spectrum for the side mode in Fig. 2 has qualitatively different features compared to those shown in Fig. 1. These can be understood by noting that the enhancement term in (30) is relatively small. The RIN spectrum is therefore approximately Lorentzian with a width $\sim \Gamma_s$. As seen from (14), Γ_s has two distinct contributions arising from spontaneous emission and nonlinear-gain suppression. For $S/P = 10^{-5}$, the contribution of spontaneous emission dominates, and $\Gamma_s \simeq R_{sp}/S \sim 1$ THz; as a result, RIN remains constant on the frequency scale of Fig. 1 ($\omega \ll \Gamma_s$). For $S/P \geq 10^{-3}$, the nonlinear-gain contribution to Γ_s starts to dominate; this results in the high-frequency drop off seen in Fig. 1. Note that in Fig. 1 the low-frequency noise first increases and then decreases as the side mode grows. This can also be understood from (14) and (30). For $S/P < 10^{-3}$, $\Gamma_s \simeq R_{sp}/S$, and RIN $\propto S$. However, Γ_s becomes proportional to S for $S/P > 10^{-2}$, and therefore RIN $\propto S^{-3}$. The second term in (30) is responsible for the slight enhancement near the relaxation-oscillation frequency.

We now consider the RIN for the total intensity in both modes. Using (22), (23), and (6), we obtain

$$
\frac{\langle | \tilde{p} + \tilde{s} |^2 \rangle}{(P + S)^2}
$$

$$
= \frac{2R_{sp}P(\Gamma_n^2 + \omega^2)}{(P + S)^2 |D(\omega)|^2} \left[\left| 1 - \frac{\Omega_R^2(S/P)}{(\Gamma_n + i\omega)(\Gamma_s + i\omega)} \right|^2 \right.
$$

$$
\left. + \frac{\Gamma_p^2 + \omega^2}{\Gamma_s^2 + \omega^2} \frac{S}{P} \right] . \tag{31}
$$

The total RIN as a function of the frequency was calculated using (31) and was found to be nearly independent of the mode-suppression ratio S/P. The RIN spectrum nearly coincides with the main-mode RIN curve for $S/P = 10^{-5}$ in Fig. 1 for all values of $S/P < 0.1$. As one may expect, the selective enhancement of the main-mode noise is due to anticorrelation between the two modes. This can be seen more clearly by calculating the cross-spectral density given by

$$
\langle \tilde{p}(\omega)\tilde{s}^*(\omega) \rangle = -2R_{sp}S \left[\frac{\Gamma_n + i\omega}{\Gamma_s + i\omega} \frac{\Omega_R^2}{|D|^2} \right.
$$

$$
\left. + \frac{\Omega_R^2}{D(\Gamma_s^2 + \omega^2)} \right] . \tag{32}
$$

The second term in (32) provides the dominant contribution. Negative values of the cross-spectral density imply anticorrelation between the two modes.

The effect of nonlinear gain on the RIN spectra was investigated by changing the parameter β. An increase in β reduces the height of resonance peak in Fig. 1 because of a faster decay of relaxation oscillations. If the nonlinear-gain effects are neglected by setting $\beta = 0$, the peak height in Fig. 1 increases by about 10 dB. To study the effect of
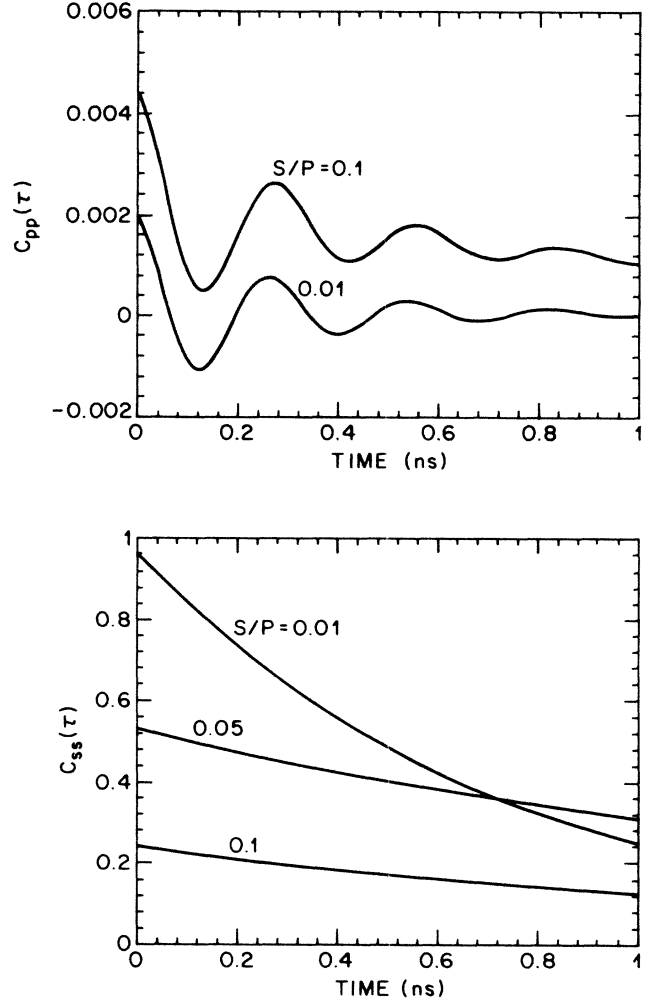

FIG. 2. Autocorrelation functions for the main mode (upper figure) and the side mode (lower figure) as a function of τ for several values of S/P.

cross saturation, the ratio θ/β was varied. Since (29) and (30) are independent of θ, the exact solutions (20) and (21) were used to calculate the RIN spectra. The RIN changed by less than a few percent as θ/β was varied in the range $0 - 2$. The negligible dependence of the RIN on θ justifies our approximations made in the derivation of the analytic solutions (29) and (30).

IV. INTENSITY AUTOCORRELATION

The solution (22) and (23) for intensity fluctuations can be used to obtain autocorrelation functions for the main and side modes defined (in the normalized form) by

$$
C_{pp}(\tau) = \langle p(t + \tau)p(t) \rangle / P^2 , \tag{33}
$$

$$
C_{ss}(\tau) = \langle s(t + \tau)s(t) \rangle / S^2 . \tag{34}
$$

From the Wiener-Khinchin theorem,[23] the autocorrelation function is related to the Fourier transform of the

spectral density, i.e.,

$$C_{pp}(\tau) = \frac{1}{2\pi} \int_{-\infty}^{\infty} \frac{\langle |\tilde{p}(\omega)|^2 \rangle}{P^2} \exp(i\omega\tau)d\tau , \qquad (35)$$

$$C_{ss}(\tau) = \frac{1}{2\pi} \int_{-\infty}^{\infty} \frac{\langle |\tilde{s}(\omega)|^2 \rangle}{S^2} \exp(i\omega\tau)d\tau . \qquad (36)$$

We can evaluate $C_{pp}(\tau)$ and $C_{ss}(\tau)$ using (29) and (30) and performing the integration using the method of contour integration. By closing the contour in the upper half-plane, we note that the contour encloses three simple poles located at $\omega = i\Gamma_s$, $\omega = \Omega_R + i\Gamma_R$, and $\omega = -\Omega_R + i\Gamma_R$. Since the algebra, although tedious, is straightforward, we write the final result given by

$$C_{pp}(\tau) = \frac{R_{\rm sp}}{P} \left[\frac{\exp(-\Gamma_R\tau)}{2\Gamma_R}\mathrm{Re}\left[\frac{\Omega_R^2 + \Gamma_n^2 - \Gamma_R^2 + 2i\Omega_R\Gamma_R}{\Omega_R(\Omega_R + i\Gamma_R)}\exp(i\Omega_R\tau) \right] \right.$$

$$\left. + \frac{S}{P}\left[\frac{a\exp(-\Gamma_s\tau)}{\Gamma_s} + \frac{b\exp(-\Gamma_R\tau)}{2\Gamma_R} \right] \right] , \qquad (37)$$

$$C_{ss}(\tau) = \frac{R_{\rm sp}}{S} \left[\frac{\exp(-\Gamma_s\tau)}{\Gamma_s} + \frac{S}{P}\left[\frac{a\exp(-\Gamma_s\tau)}{\Gamma_s} + \frac{b\exp(-\Gamma_R\tau)}{2\Gamma_R} + \right] \right] , \qquad (38)$$

where

$$a = \frac{\Omega_R^4}{|\Omega_R + i(\Gamma_R + \Gamma_s)|^2 |\Omega_R + i(\Gamma_R - \Gamma_s)|^2} , \qquad (39)$$

$$b = \mathrm{Re}\left[\frac{\Omega_R^3 \exp(i\Omega_R\tau)}{(\Omega_R + i\Gamma_R)[\Omega_R + i(\Gamma_R + \Gamma_s)][\Omega_R + i(\Gamma_R - \Gamma_s)]} \right] , \qquad (40)$$

and Re stands for the real part of the expression in parentheses.

Equations (37) and (38) show the autocorrelation function consists of three exponentially decaying terms. The terms decaying as $\exp(-\Gamma_R\tau)$ are due to the contribution from relaxation oscillations while side-mode fluctuations contribute as terms proportional to $\exp(-\Gamma_s\tau)$. The last two terms proportional to S/P in (37) and (38) vanish if each mode fluctuates independently of the other. In general, however, the two modes are coupled, and the autocorrelation depends on the mode-suppression ratio. Figure 2 shows the dependence of $C_{pp}(\tau)$ and $C_{ss}(\tau)$ on the intensity ratio S/P. Note that $C_{pp}(\tau)$ increases with an increase in S/P and shows an oscillatory structure related to relaxation oscillations. By contrast, $C_{ss}(\tau)$ does not oscillate and decreases rapidly with an increase in S/P.

As seen from (33) and (34), the autocorrelation functions provide noise variance for $\tau = 0$, i.e.,

$$\sigma_p^2/P^2 = C_{pp}(0), \quad \sigma_s^2/S^2 = C_{ss}(0) \qquad (41)$$

where σ_p^2 and σ_s^2 represent the noise variance for the main and side modes, respectively. We can obtain simple analytic expressions for them if we assume that all decay rates are small in comparison to Ω_R. Using (37) and (38) in (41), we obtain

$$\left[\frac{\sigma_p}{P}\right]^2 \simeq \frac{R_{\rm sp}}{P\Gamma_p}\left[1 + \frac{S}{P}\left[1 + \frac{\Gamma_p}{\Gamma_s}\right]\right] , \qquad (42)$$

$$\left[\frac{\sigma_s}{S}\right]^2 \simeq \frac{R_{\rm sp}}{S\Gamma_s}\left[1 + \frac{S}{P}\left[1 + \frac{\Gamma_s}{\Gamma_p}\right]\right] , \qquad (43)$$

where we have replaced $2\Gamma_R$ by Γ_p by noting that $\Gamma_n \ll \Gamma_p$ in (27). It is important to realize that Γ_p and Γ_s themselves depend on P and S as shown in (13) and (14).

As one may expect, the main-mode noise σ_p increases with the growth of the side mode. By contrast, the noise-to-signal ratio σ_s/S for the side mode decreases rapidly with an increase in S/P. It can be shown[4] that for a weak side mode oscillating independently of the main mode, fluctuations obey an exponential distribution, a characteristic signature of chaotic light. For such a distribution $C_{ss}(0) = 1$. As seen in Fig. 2, $C_{ss}(0)$ approaches 1 for only very weak side modes such that $S/P < 10^{-2}$. The physical mechanism behind this departure is the nonlinear gain. For $S/P < 10^{-2}$, $\Gamma_s \simeq R_{\rm sp}/S$. It then follows from (43) that $\sigma_s/S \simeq 1$. However, the dominant contribution to σ_s/S decreases as S^{-1} for $S/P > 0.05$ since $\Gamma_s \simeq \beta_{22}S$ from (14). Although σ_s has been measured,[24] the contribution of the nonlinear gain remained unidentified because of the finite filter bandwidth (or a relatively large sampling window) that also results in a reduction of σ_s/S. Further, the nonlinear-gain effects are expected to be less important for the ridge-waveguide structure employed in the experiment.

V. INTENSITY CROSS CORRELATION

As mentioned earlier, mode-partition noise is a manifestation of anticorrelation between the two modes. A normalized measure of this anticorrelation is provided by the cross-correlation function defined as[23]

$$C_{ps}(\tau) = \langle p(t+\tau)s(t)\rangle/PS$$

$$= \frac{1}{2\pi}\int_{-\infty}^{\infty}\frac{\langle \tilde{p}(\omega)\tilde{s}^*(\omega)\rangle}{PS}\exp(i\omega\tau)d\tau , \quad (44)$$

where the cross-spectral density is given by (32). The integration can be performed using the method of contour integration. The result is

$$C_{ps}(\tau) = \frac{R_{\text{sp}}}{P}\left[-\frac{\exp(-\Gamma_s\tau)\Omega_R^2}{\Gamma_s[\Omega_R^2+(\Gamma_R-\Gamma_s)^2]} - \frac{2\exp(-\Gamma_R\tau)}{\Omega_R}\text{Im}\left[\frac{\Omega_R^2\exp(i\Omega_R\tau)}{\Omega_R^2+\Gamma_s^2-\Gamma_R^2+2i\Omega_R\Gamma_R}\right]\right.$$

$$\left. +\frac{\exp(-\Gamma_R\tau)}{2\Gamma_R}\text{Re}\left[\frac{\Omega_R[\Omega_R+i(\Gamma_R-\Gamma_n)]\exp(i\Omega_R\tau)}{(\Omega_R+i\Gamma_R)[\Omega_R+i(\Gamma_R+\Gamma_s)]}\right]\right] . \quad (45)$$

Figure 3 shows the variation of C_{ps} with τ for three values of the ratio S/P; the oscillatory structure is due to the contribution of relaxation oscillations governed by the last two terms in (45).

The value of the cross-correlation function at $\tau=0$ is related to the mode-partition coefficient[15] k by the simple relation

$$k^2 = -C_{ps}(0) . \quad (46)$$

If we use (45) and make the simplifying approximation that $\Omega_R \gg \Gamma_R$ and Γ_s, we obtain

$$k^2 \simeq \frac{R_{\text{sp}}}{P\Gamma_s}\left[1-\frac{\Gamma_s}{2\Gamma_R}\right] . \quad (47)$$

Equation (47) provides a simple analytic expression for the mode-partition coefficient in a two-mode laser. It differs from a previous estimate[11] obtained assuming an exponential distribution for the side-mode intensity. It can be reduced to that if (i) we neglect the second term in (47) arising from relaxation oscillations and (ii) neglect the contribution of the nonlinear gain to Γ_s. Under these approximations, $\Gamma_s = R_{\text{sp}}/S$, and (47) reduces to $k^2 = S/P$. When the nonlinear-gain contribution to Γ_s dominates ($S/P > 0.05$), we can approximate $\Gamma_s \simeq \beta_{22}P$ and $\Gamma_p \simeq \beta_{11}P$ using (13) and (14). Using these values in (47), $\beta=\beta_{11}\simeq\beta_{22}$, and $\Gamma_R \simeq \Gamma_p/2$ we obtain

$$k^2 \simeq \frac{R_{\text{sp}}}{\beta PS}\left[1-\frac{S}{P}\right] . \quad (48)$$

We can estimate the mode-partition coefficient k using (47) and Table I. For a mode-suppression ratio of 20 dB, $k\simeq0.09$ but becomes 0.14 when the side-mode suppression is 10 dB. Such values of k are consistent with the experimental measurements on distributed-feedback lasers.[12]

VI. CONCLUSIONS

In order to analyze the effect of a weak side mode on the noise characteristics of a dominantly single-longitudinal-mode semiconductor laser, we have solved the Langevin rate equations using a two-mode model. This has allowed us to obtain analytic expressions for the spectral densities and the correlation functions associated with the two modes.

We have obtained simple analytic expressions for the noise variances σ_p and σ_s of the main and side modes. These results show that σ_s/S deviates significantly from 1, a value expected if the side-mode intensity has an exponential distribution corresponding to that of chaotic light. We have also obtained a simple expression for the mode-partition coefficient by relating it to the cross-correlation function. In the absence of the nonlinear-gain contribution, our result reduces to that obtained previously. The analysis presented here emphasizes that mode-partition noise depends on the mode-suppression ratio as well as on the nonlinear-gain parameters. The relatively small values of the mode-partition coefficient imply that mode-partition noise should not be a limiting factor for the performance of single-frequency lasers as long as side modes are suppressed by about a factor of 100. This is consistent with previous experimental and theoretical results.[4,7,10]
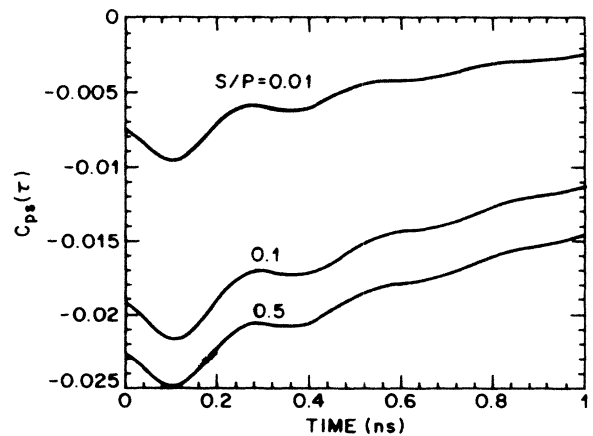

FIG. 3. Cross-correlation function $C_{ps}(\tau)$ as a function of τ for three values of S/P. The oscillatory structure is due to relaxation oscillations.

[1]H. Jäckel and G. Guekos, Opt. Quantum Electron. **9**, 233 (1977).

[2]G. Arnold and K. Petermann, Opt. Quantum Electron **12**, 207 (1980).

[3]R. Schimpe, Z. Phys. B **52**, 289 (1983).

[4]C. H. Henry, P. S. Henry, and M. Lax, J. Lightwave Technol. **LT-2**, 209 (1984).

[5]P.-L. Liu and K. Ogawa, J. Lightwave Techol. **LT-2**, 44 (1984).

[6]D. Marcuse, IEEE J. Quantum Electron. **QE-20**, 1148 (1984).

[7]R. A. Linke, B. L. Kasper, C. A. Burrus, I. P. Kaminow, J.-S. Ko, and T. P. Lee, J. Lightwave Technol. **LT-3**, 706 (1985).

[8]G. L. Abbas and T. K. Yee, IEEE J. Quantum Electron, **QE-21**, 1303 (1985).

[9]R. Schimpe, Proc. Inst. Electr. Eng. Part J **132**, 146 (1985).

[10]T. M. Shen and G. P. Agrawal, Electron Lett. **21**, 1220 (1985).

[11]E. E. Basch, R. F. Kearns, and T. G. Brown, J. Lightwave Technol. **LT-4**, 516 (1986).

[12]S. Yamamoto, H. Sakaguchi, and N. Seki, J. Lightwave Technol. **LT-4**, 672 (1986).

[13]N. H. Jensen, H. Olesen, and K. E. Stubkjaer, IEEE J. Quantum Electron. **QE-23**, 71 (1987).

[14]H. Akabane, T. Tsuchiya, T. Kawakubo, and H. Abe, Jpn. J. Appl. Phys. **24**, L501 (1985).

[15]K. Ogawa, in *Semiconductor and Semimetals*, Vol. 22C, edited by W. T. Tsang (Academic, New York, 1985).

[16]R. S. Tucker, J. Lightwave Technol. **LT-3**, 1180 (1985).

[17]J. Manning, R. Olshansky, D. M. Fye, and W. Powazinik, Electron. Lett. **21**, 496 (1985).

[18]G. P. Agrawal, IEEE J. Quantum Electron. **QE-23**, 860 (1987).

[19]D. E. McCumber, Phys. Rev. **141**, 306 (1966).

[20]M. Lax, Rev. Mod. Phys. **38**, 541 (1966).

[21]M. Lax, Phys. Rev. **160**, 290 (1967).

[22]C. H. Henry, J. Lightwave Technol. **LT-4**, 298 (1986).

[23]J. W. Goodman, *Statistical Optics* (Wiley, New York, 1985).

[24]P. L. Liu, J. Lightwave Tech. **LT-3**, 205 (1985).